Egyptian Journal of Cell and Tissue Research
Print ISSN: 2812-5436 / Online ISSN: 2812-5444

Comparative Histological Study of the Possible Protective Effect of Valsartan Versus Dexamethasone On Cyclophosphamide-Induced Lung Injury in Adult Male Albino Rat

Fatma Elzahraa Mohammed Abdel Lattif, Dalia Hussein Abdel Aziz, Doha Hassan Mohammed Ahmed, Gaber Fekry Genedy.

Department of histology, Faculty of Medicine, Beni-Suef University,Egypt

Abstract:

Introduction: Interstitial lung diseases are groups of chronic lung diseases characterized by inflammation and fibrosis. **Aim of work:** The present study was performed to evaluate the possible protective effect of valsartan versus dexamethasone on cyclophosphamide-induced lung injury in adult male albino rat. **Material and Methods:** Thirty male albino Rats were divided into 6 groups; 5 rats each: group I (Control), group II (Cyclophosphamide), group III (Valsartan), group IV (Dexamethasone), group V (Dexamethasone & Cyclophosphamide), and group VI (Valsartan and Cyclophosphamide). Lung specimens were taken on the 6th day of experiment. Specimens were subjected to histological (Hematoxylin and Eosin, Periodic Acid-Schiff, and Masson's trichrome) and immunohistochemical (Alpha smooth muscle actin, Clsuter of Differentiation 86, and inducible Nitric Oxide Synthase) studies. Also, morphometric studies and statistical analysis were done. **Results:** Features of acute lung injury appeared in group II as thickening of interalveolar septa, narrowing of alveoli, and cellular infiltrations. There were significant increases in the mean area percentage of collagen fibers, inducible Nitric Oxide Synthase and Alpha smooth muscle actin, besides significantly increased number of Periodic Acid-Schiff -positive goblet cells and alveolar macrophages in anti- Clsuter of Differentiation 86 immuostained sections, and thickness of interalveolar septa. Sections in group V and group VI demonstrated that lung tissue restored normal histological and immunohistochemical results, compared to group II. There was a significant decrease in mean area percentage of collagen fibers, inducible Nitric Oxide Synthase and Alpha smooth

muscle actin, number of Periodic Acid-Schiff -positive goblet cells and alveolar macrophages in anti- Clsuter of Differentiation 86 immuostained sections, and thickness of interalveolar septa as compared to group II. **Conclusion:** valsartan and dexamethasone possess protective effects against cyclophosphamide induced lung toxicity with the upper hand was to valsartan.
Keywords: Cyclophosphamide, Valsartan, Dexamethasone, Lung, Rat.

1. Introduction:

Interstitial lung diseases (ILDs) are groups of chronic lung diseases characterised by varying degrees of inflammation and fibrosis. Inhaled toxic agents such as silica, non-inhaled toxic agents such as chemotherapeutics, irradiation, viral agents and autoimmune illnesses can all induce ILD. It can also be caused by an unknown source, as in idiopathic pulmonary fiprosis, the most frequent ILD with the worst prognosis [(1)].

The COVID-19 pandemic rapidly spread around the world following the first reports in Wuhan City, China in late 2019. The disease, caused by the novel SARS-CoV-2 virus, is primarily a respiratory condition that can affect numerous other systems including the cardiovascular and gastrointestinal systems. The disease ranges in severity from asymptomatic to severe acute respiratory distress requiring intensive care treatment and mechanical ventilation, which can lead to respiratory failure and death. It has rapidly become evident that COVID-19 patients can develop features of interstitial pulmonary fibrosis (IPF) [(2)].

Cyclophsphamide (CP) is an antineoplastic alkylating agent extensively used for treating various malignancies including lymphoma, leukemia and breast cancer. Injuries of normal tissues beside other side effects as damage to the kidney and thyroid cancer have been reported as a result of widespread usage of CP. CP-induced lung injury is similar to interstitial pulmonary fibrosis caused by the novel SARS-CoV-2 virus [(1)].

Valsartan is Angiotensine II Receptor Type 1 antagonist has been widely used in the treatment of diseases like hypertension, heart failure, myocardial infarction and diabetic neuropathy. Its beneficial effects are related to the inhibition of angiotensin II by blockage of AT1 receptor (Angiotensine II Receptor Type 1) [(3)].

Dexamethasone (DEXA) is a potent long lasting synthetic glucocorticoid known to inhibit the inflammatory cascade because of its potent anti-inflammatory effects. It is widely used to treat a variety of acute and chronic inflammatory diseases including

acute lung inflammation, asthma and rheumatoid arthritis [4].

The aim of the current study was to compare between the effects of valsartan versus dexamethasone on cyclophosphamide-induced lung injury in adult male albino rat.

2. Materials and Methods:

Animals:

Thirty male adult albino rats 5-6 months old ,weighing 200-250 g were used in this study .Each group was housed in a separate cage in a constant temperature (22-24° C) and light-controlled room on an alternating 12:12 h light dark cycle and have free access to food. Rats were fed a standard commercial pellet diet and kept for one week before starting the experiment for acclimatization. The study was conducted in pharmacology lab, Faculty of Medicine, Beni-Suef University. The study was executed in compliance with the ethical guidelines and policies approved by the Animal Care and Use Committee of Faculty of Medicine, Beni-Suef University and complies with the Guide for the Care and Use of Laboratory Animals (Approval number:021-169). All measures were taken to decrease the number of animals used and lessen animal suffering.

Chemicals:

Valsartan (VAL): Tareg (valsartan) 80 mg film coated tablets, from NOVARTIS Pharma S.A.E. Cairo; each tablet was dissolved in 10 ml distilled water. Each rat received VAL (15mg/kg/day) orally by nasogastric tube for 6 days.

Dexamethasone (DEX): 8mg Vial from NOVARTIS Pharma S.A.E. Cairo. Each rat received dexamethasone (5mg/kg/day) intraperitoneal injection for 6 days.

Cyclophosphamide (CP): 1g dry powder from NOVARTIS Pharma S.A.E. Cairo was diluted with normal saline 0.9 %. Each rat received CP (200mg/kg) intraperitoneal injection, single dose on day 6.

Experimental Design:

The animals will be divided into 6 groups (5 rats each):

Group I (control): Each rat received distilled water (2ml/kg/day) orally by nasogastric tube for 6 days.

Group II (cyclophosphamide): Each rat received distilled water (2ml/kg/day) orally by nasogastric tube for 6 days. Then CP (200mg/kg) by intraperitoneal injection, single dose on day 6 [5].

Group III (Valsartan): Each rat received VAL (15 mg/kg/ day) orally by nasogastric tube for 6 days [5].

Group IV (DEX): Each rat received dexamethasone (5mg/kg/day) intraperitoneal injection for 6 days [4].

Group V (DEX +CP): Each rat received dexamethasone (5mg/kg/day)

intraperitoneal injection for 6 days and CP (200mg/kg) intraperitoneal injection, single dose on day 6 [4].

Group VI (Valsartan + CP): Each rat received VAL (15 mg/kg/day) orally by nasogastric tube for 6 days and CP (200mg/kg.) intraperitoneal injection, single dose on day 6 [1].

At the 6th day of the experiment, rats were anesthetized with ketamine and subjected to cervical dislocation. Afterwards, lung was rapidly separated and washed with saline, then rapidly fixed in 10% neutral buffered formalin and processed for paraffin sections of 5-7 µm thickness. These sections were subjected to the following:

1- Hematoxylin and Eosin (H&E) for histological examination [6].

2- PAS stain for detection of goblet cells in the epithelial lining of bronchi [7].

3- Masson's Trichrome stain for detection of collagen fibers [7].

4- Immunohistochemical staining for Alpha smooth muscle actin antibody (αSMA) [7], Clsuter of Differentiation 68 antibody (CD68) [6], and Inducible Nitric Oxide Synthase antibody (iNOS) [8].

For αSMA staining_all specimens were processed routinely, slides were kept in 1.5% hydrogen peroxide and in methanol for 15 minutes, then slides were rinsed for 5 minutes in phosphate buffer saline , then sections for immunohistochemical stains were boiled for 10 min in 10 mM citrate buffer (AP9003) at pH 6 for antigen retrieval then incubated for 1h with about 2 drops or 100 µl for each section from the primary antibody. αSMA was the Primary antibody which is a mouse monoclonal antibody (Thermo Fischer scientific, CA, USA, catalogue number MS-113-R7) then detection was performed using a HRP-conjugated secondary antibody followed by colorimetric detection using a DAB kit. Ultravision detection system (TP-015-HD) was used to complete immunostaining and Mayer'shematoxylin (TA060-MH) was used for counterstaining. Citrate buffer, Ultravision detection system and Mayer's hematoxylin were purchased from Labvision Thermo Scientific, Fremont, California, USA. Negative controls were done by applying the same steps but omitting the step of adding the primary antibodies. Positive reaction in the specimen of human uterus appears as brown deposits in the cytoplasm of αSMA (positive) cells.

For iNOS staining, all specimens were processed routinely, slides were kept in 1.5% hydrogen peroxide and in methanol for 15 minutes, then slides were rinsed for 5 minutes in phosphate buffer saline, then antigen retrieval was performed by incubating the sections in 1mmol/L ethylene

diamine triacetic acid (EDTA), PH 8.0 placed in water bath at 95−98°C (not boiling) for 30 minutes and then removed from the bath and allowed to cool for 20 minutes, then incubated for 1h with about 2 drops or 100 µl for each section from the primary antibody. iNOS was the Primary antibody which is a rabbit polyclonal antibody recognizing iNOS (Product # PA1-036), Transduction Laboratories, San Diego, California, USA) detection was performed using a biotin-conjugated secondary antibody and SA-HRP, followed by colorimetric detection using DAB. Ultravision detection system (TP-015-HD) was used to complete immunostaining and Mayer'shematoxylin (TA060-MH) was used for counterstaining. Citrate buffer, Ultravision detection system and Mayer's hematoxylin were purchased from Labvision Thermo Scientific, Fremont, California, USA. Negative controls were done by applying the same steps but omitting the step of adding the primary antibodies. Positive reaction in the specimen of human heart appears as brown deposits in the cytoplasm of iNOS (positive) cells.

For CD68 staining (using the avidin–biotin–peroxidase method), all specimens were processed routinely. Briefly, paraffin sections of 4-µm thickness were dewaxed in xylene, rehydrated in descending series of ethanol, and immersed in 0.3% H2O2 for 30 min to block endogenous peroxidase. After microwaving of samples for 15 min in citrate buffer (pH 6.0), antigens were retrieved. 10% goat serum (Dako Ltd, Cambridgeshire, UK) was used for 30 min to block non-specific binding. Tissue sections were rinsed gently with PBS and sections were incubated overnight at 4 °C with CD68 antibody (mouse monoclonal antibody, 1:200 dilutions, code NCL-L-CD68; Leica Biosystems, Benton La, Newcastle Ltd, UK). The sections were incubated with biotinylated CD68 anti-mouse immunoglobulin (Dako Ltd) for the corresponding primary antibody and thereafter sections were incubated with the avidin–biotin–horseradish peroxidase complex according to the manufacturer's instructions (ABC kit from Vector Laboratories Ltd. UK). Peroxides were visualized by incubating the sections in diaminobenzidine (Sigma Chemical Co., Poole, UK) and H2O2 and counterstained with Mayer's hematoxylin, dehydrated and mounted with DPX. Negative controls were obtained by neglecting the incubation with the primary antibody. Positive reaction in the specimen of human tonsil appears as brown deposits in the cytoplasm of CD68 (positive) cells.

Morphometric study

The following parameters were measured

1-Measurement of the thickness of interalveolar septa in 10 non-overlapping fields of H&E stained sections (n=10) at 400×magnifcation in all groups.

2-Measurement of the mean area percentage of αSMA immune-stained smooth muscle,collagen fibers and iNOS positive cells at 200×magnifcation in all groups.

3-Measurement of the mean number of PAS-positive goblet cells per bronchiole and mean number of alveolar macrophages in anti-CD68 immunostained sections at 200×magnifcation in all groups.

Data were obtained using *"Leica Qwin 500 C"* image analyzer computer system Ltd. (Cambridge, England). (Histopathology Department, Faculty of veterinary Medicine, Beni-Suef University).

All these morphometrically measured data were statistically analyzed.

Statistical Methods

All data are quantitative variables, and were illustrated as mean±standard error of mean (SEM). One-way ANOVA test/Tukey's *post hoc* analysis for pairwise comparisons was done to detect significance between groups.

When *P* value =0.05, significance is set. GraphPad Prism computer software version 8 was used to carry out the statistical procedures (9).

(A)Histological results:

(1) Hematoxylin and Eosin: Fig (1)

Examination of H&E stained sections of the lung of group I (control) revealed that normal histological architecture with patent alveoli separated by thin interalveolar septa Fig(1a). In group II (CP treated), lung tissues showed thickening of the interalveolar septum and the walls of bronchioles were expanded by cellular infiltrate, exfoliated epithelium and inflammatory exudate in the lumen of the bronchiole_Fig (1b). In groupIII (Valsartan treated) and group IV (DEXA treated) showed the normal histological architecture of the lung tissue with variable sized patent alveoli, separated by thin interalveolar septa Figs (1c,d) .In group V (CP + Dexa treated partial restoration of the normal lung tissue appeared through which some alveoli appeared normal while others are narrowed and the bronchioles showed folded mucosa Fig (1e). In group VI (CP +Valsartan) showed that many alveoli and interalveolar septa restored their normal architecture with mild cellular infiltration of the interstitium Fig (1f).

(2) The periodic acid-Schiff (PAS) stain Fig (2)

Examination of PAS stained lung sections of group I (control) showed few goblet cells in the lung bronchiole Fig (2a).In group II (CP treated), showed numerous PAS positive

goblet cells in the lung bronchiole Fig (2b). In groupIII (Valsartan treated) and group IV (DEXA treated) showed few PAS positive goblet cells in the lung bronchiole Fig (2c, d) .In group V (CP + Dexa treated) and group VI (CP +Valsartan) showed few PAS positive goblet cells in the lung bronchiole Fig (2e,f).

(3) Masson's trichrome stained sections: Fig (**3**)

Examination of Masson's trichrome stained lung sections of group I (control group) showed fine collagen fibers in the interalveolar septa Fig (3a).In group II (CP treated) showed deposition of collagen fibers in the wall of blood vessel and in the thickened interalveolar septa Fig (3b). In groupIII (Valsartan treated) and group IV (DEXA treated) showed fine collagen fibers in the interalveolar septa Fig (3c, d) .In group V (CP + Dexa treated) and group VI (CP +Valsartan) showed moderate deposition of collagen fibers in the interalveolar septa Fig (3e, f).

(4) α SMA immunohistochemical stained sections: Fig(4)

Examination of α SMA stained lung sections of group I (control group) showed negative α SMA reaction in the wall of alveoli and interalveolar septa while positive in the smooth muscles investing bronchioles Fig (4a). In group II (CP treated) sections showed strong positive cytoplasmic reaction in the wall of alveoli and interalveolar septa Fig (4b). In groupIII (Valsartan treated) and group VI (CP +Valsartan) showed weak cytoplasmic immunoreactivity for α SMA in the wall of blood vessel Fig (4c,f) .Lung sections in group IV (DEXA treated) and group V (CP + Dexa treated) DEXA treated groups showed moderate cytoplasmic immunoreactivity for αSMA in the wall of bronchiole Fig (4d,e) .

(5) CD68 immunohistochemical stained sections: Fig (5)

Examination of CD68 stained lung sections of group I (control group) showed negative CD68 alveolar macrophages in the interalveolar septa Fig (5a). In group II (CP treated) sections showed moderate positively stained CD68 alveolar macrophages within the interalveolar septa Fig (5b). In groupIII (Valsartan treated) and group IV (DEXA treated) showed negative CD68 alveolar macrophages in the interalveolar septa Fig (5c,d). In group V (CP + Dexa treated) sections showed moderate positive stained CD68 alveolar macrophages in the interalveolar septa Fig (5e). In group VI (CP +Valsartan) sections showed few positive stained CD68 alveolar macrophages in the interalveolar septa Fig (5f).

(6) iNOS immunohistochemical stained sections: Fig. (6)

Examination of iNOS stained lung sections of group I (control group) showed negative iNOS expression in the interalveolar septum Fig (**6a**).In group II (CP treated) sections showed moderate iNOS immunoreactive cells within the interalveolar septum Fig (**6b**). In groupIII (Valsartan treated) and group IV (DEXA treated) sections showed negative iNOS expression in the interalveolar septum Fig (**6**c, d) .In group V (CP + Dexa treated) and group VI (CP +Valsartan) showed negative iNOS expression in the interalveolar septum Fig (**6**e,f).

(B) Morphometric and Statistical results:

Table (1**):**

Statistical analysis summary of the morphometrical parameters of the lung of all experimental groups

Fig (7)

1) The mean values of the thickness of Interalveolar septa in all experimental groups.

There was a significant increase in the thickness of interalveolar septa in group II compared to group I, while there was a significant decrease in group V and group VI in comparison with group II. Meanwhile, the thickness of interalveolar septa in group III and group IV showed a non-significant difference as compared to group I Fig (7 a).

2) The mean number of PAS-positive goblet cells per bronchiole in all experimental groups.

There was a significant increase in the mean number of PAS-positive goblet cells in group II compared to group I, while there was a significant decrease in group V and group VI in comparison with group II. Meanwhile, the mean number of PAS-positive goblet cells in group III and group IV showed a non-significant difference as compared to group I Fig (7 b).

3) The mean area percentage of masson's trichrome stained collagen fibers in all experimental groups.

There was a significant increase in the area percentage of masson's trichrome stained collagen fibers in group II compared to group I, while there was a significant decrease in group V and group VI in comparison with group II. Meanwhile, the area percentage of masson's trichrome stained collagen fibers in group III and group IV showed a non-significant difference as compared to group I Fig (7c).

(4) The mean area percentage of α-SMA immune-stained smooth muscle in all experimental groups. There was a significant increase in the area percentage of α-SMA immune-stained smooth muscle in group II compared to group I ,While there was a significant decrease in group V and

group VI in comparison with group II. Meanwhile, the area percentage of α-SMA immune-stained smooth muscle in group III and group IV showed a non-significant difference as compared to group I Fig (7 D).

(5) The mean number of alveolar macrophages in anti-CD68 immunostained sections in all experimental groups.

There was a significant increase in the mean number of alveolar macrophages in anti-CD68 immunostained sections in group II compared to group I, while there was a significant decrease in group V and group VI in comparison with group II. Meanwhile, the mean count of alveolar macrophages in anti-CD68 immunostained sections in group III and group IV showed a non-significant difference as compared to group I Fig (7 e).

6) The mean area percentage of positive iNOS immunoreactivity in anti-iNOS immunostained sections in all experimental groups.

There was a significant increase in the mean area percentage of positive iNOS immunoreactivity in anti-iNOS immunostained sections in group II compared to group I, while there was a significant decrease in group V and group VI in comparison with group II. Meanwhile, the mean area percentage of positive iNOS immunoreactivity in anti-iNOS immunostained sections in group III and group IV showed a non-significant difference as compared to group I Fig (7 f).

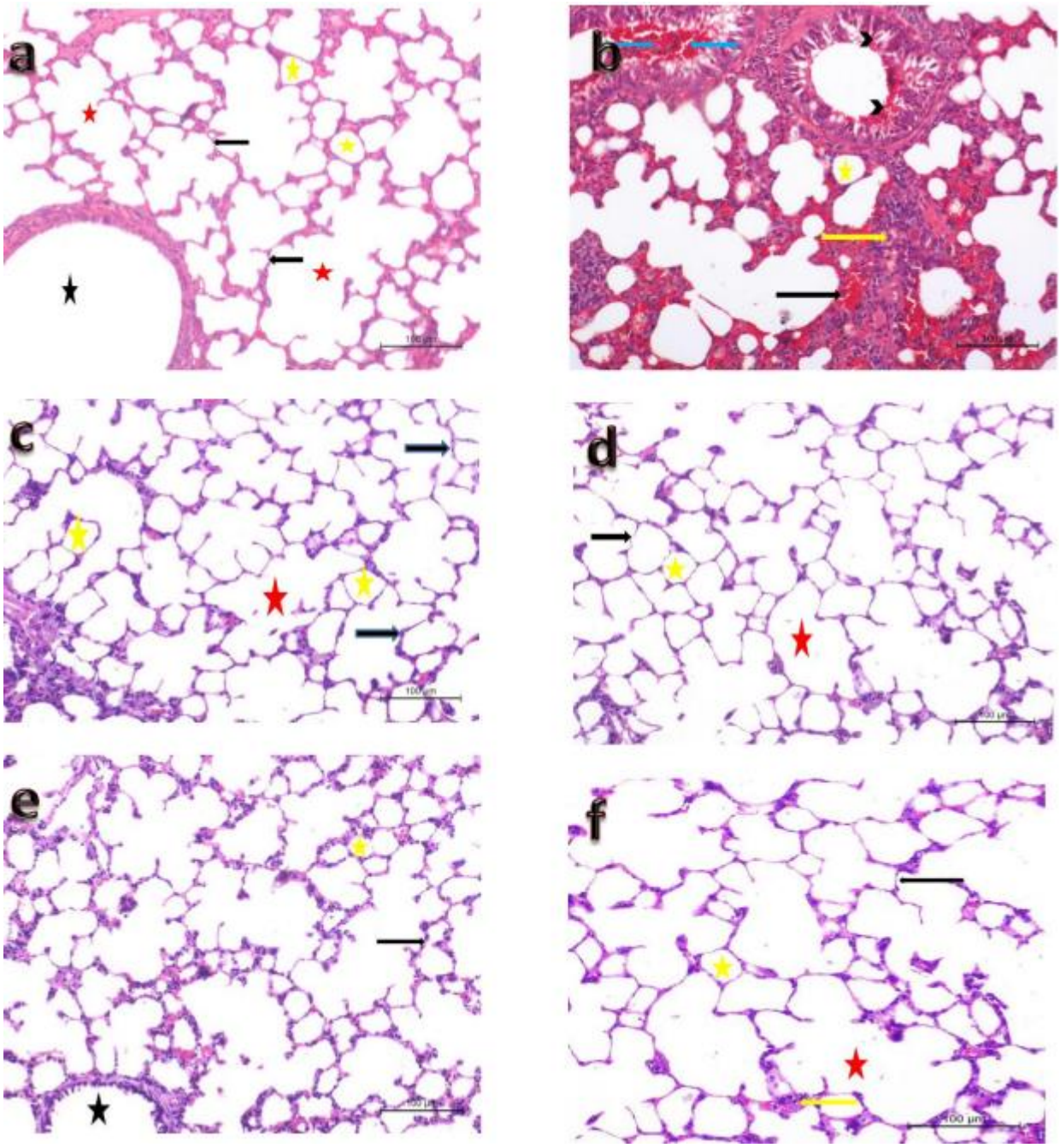

Fig (1): A photomicrograph of lung section of a rat in group I (control group)(1a) showing normal histological architecture of the lung tissue with variable sized clear patent alveoli (yellow stars), separated by thin interalveolar septa (black arrows), alveolar sacs (red star) and a patent bronchiole (black star),(1b) group II(CP group) showing thickening of the interalveolar septa (black arrow), with narrowing of the intervening alveoli (yellow star), the walls of bronchioles were expanded by cellular infiltrate (arrow head), exfoliated epithelium and inflammatory exudate in the lumen of the bronchiole (blue arrows). (1c) group III (valsartan group) showing normal histological architecture of the lung tissue with variable sized polygonal patent alveoli (yellow stars), separated by thin interalveolar septa (black arrows)and alveolar sacs (red star).(1d) group IV (Dexamethasone group) showing normal histological architecture of the lung tissue with variable sized polygonal patent alveoli (yellow stars), separated by thin interalveolar septa (black arrows) and alveolar sacs (red star).(1e) group V (CP + DEX) treated group showing bronchiole with folded

mucosa (black star), apparently thin interalveolar septum (black arrow) and some alveoli appear normal while others are narrowed (yellow stars). (1f) group VI (CP +Valsartan) treated group showing patent alveoli (yellow stars), normal alveolar sacs (red star), thin interalveolar septum (black arrow) and mild cellular infiltration of the interstitium (yellow arrow). (H&E x200).

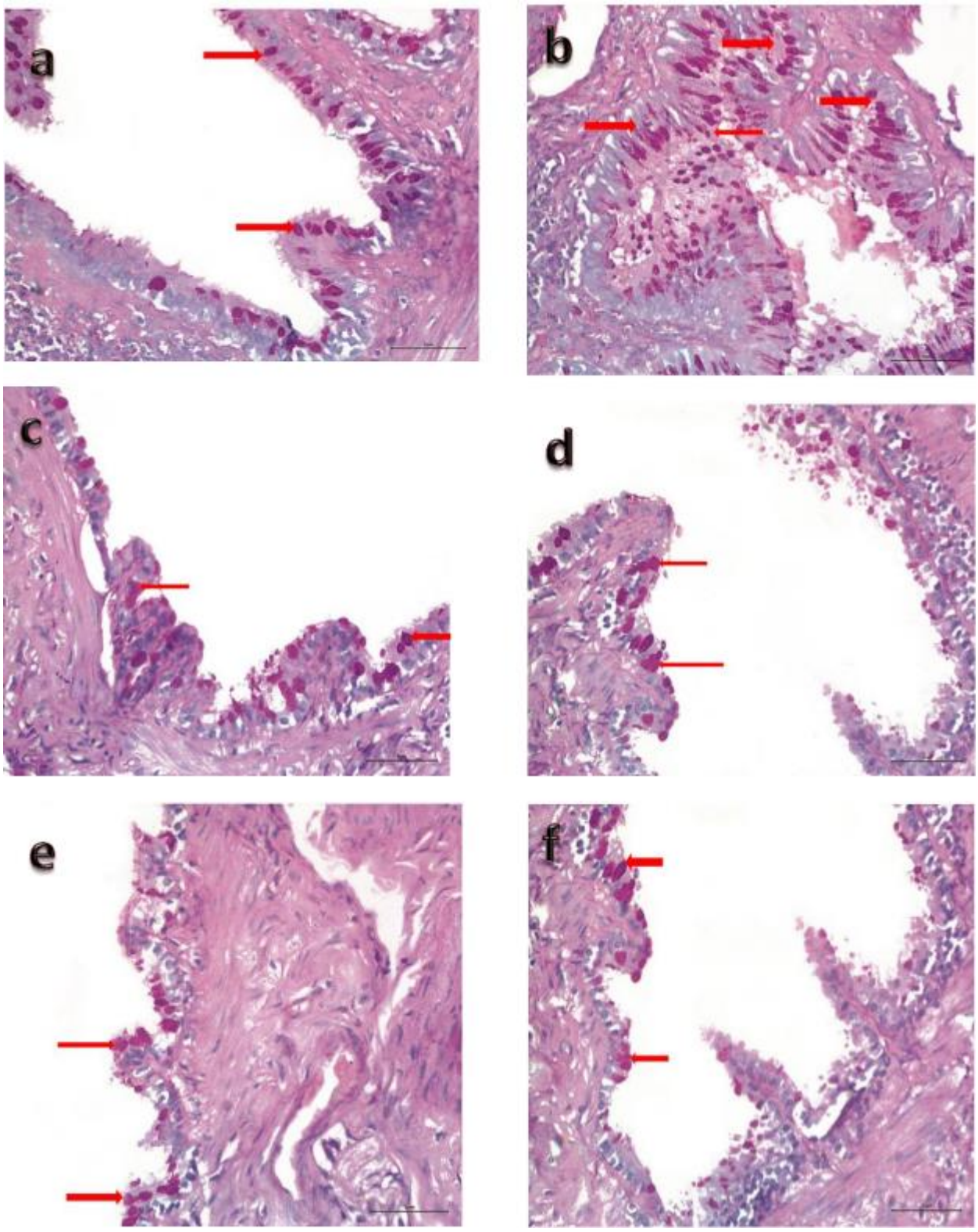

(2) The periodic acid-Schiff (PAS) stain:

Fig (2): A Photomicrograph of PAS stained lung sections of (2a): groupI control group showed few goblet cells in the lung bronchiole (red arrows). (2b): groupII (CP) treated group showed numerous PAS positive goblet cells in the lung bronchiole (red arrows). (2c): groupIII valsartan treated), (2d): groupIV (Dexa) treated, (2e): groupV (CP + DEXa) treated and (2f): groupVI (CP +Valsartan) treated groups, showed few PAS positive goblet cells in the lung bronchiole (red arrows). (PAS x400).

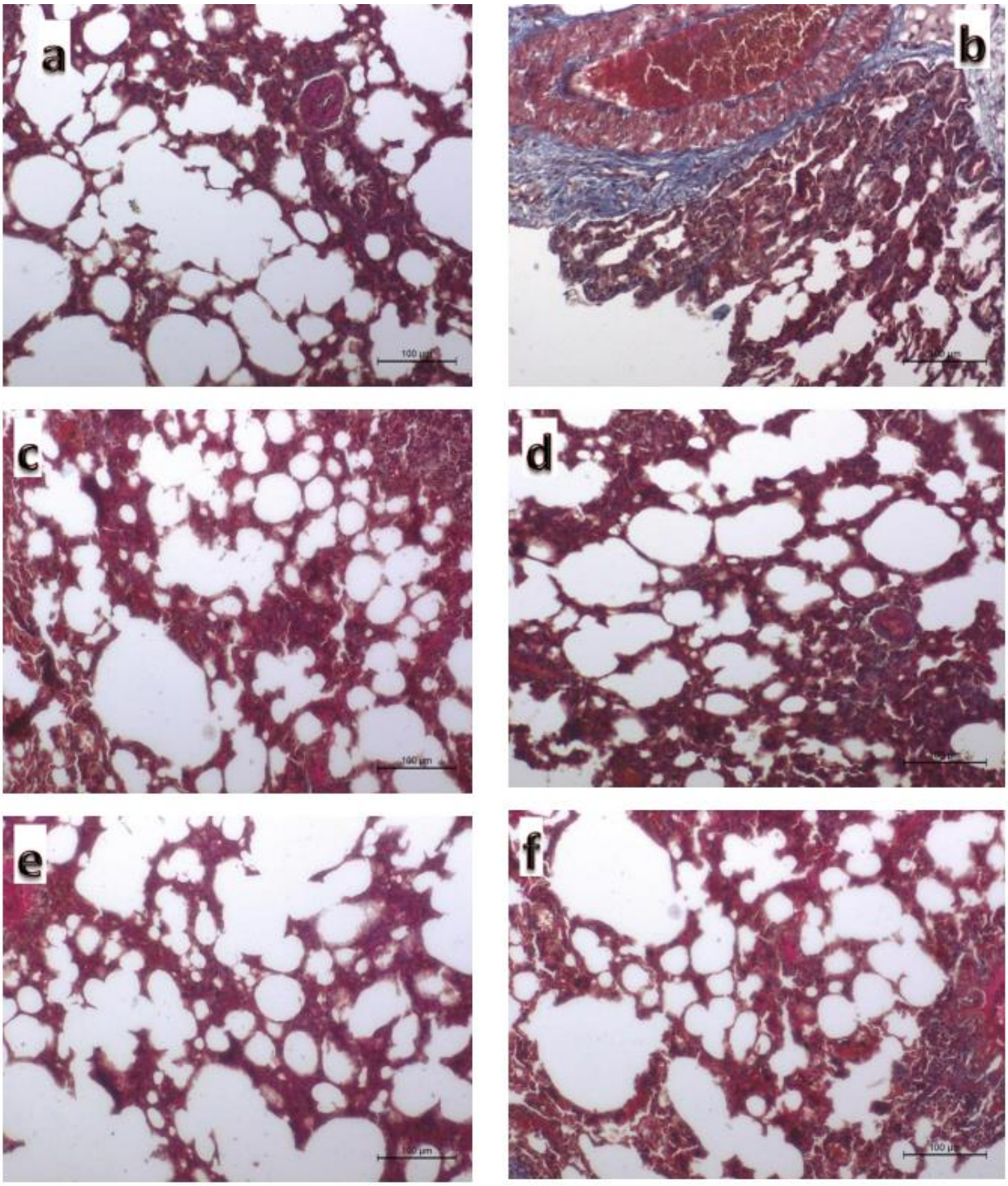

(3)Masson's trichrome stained sections:

Fig (3): A Photomicrograph of Masson's trichrome stained lung sections (3a): groupI control group showed fine collagen fibers in the interalveolar septa. (3b): groupII (CP) treated group stained lung sections showed deposition of collagen fibers in the wall of blood vessel and in the thickened interalveolar septa . (3c): groupIII valsartan treated and (3 f): groupVI (CP +Valsartan) treated groups showed fine collagen fibers in the interalveolar septa. In (3d): groupIV (Dexa) treated and (3e): groupV (CP + DEXa) treated showed fine deposition of collagen fibers in the interalveolar septa. (Masson's trichrome, x 200).

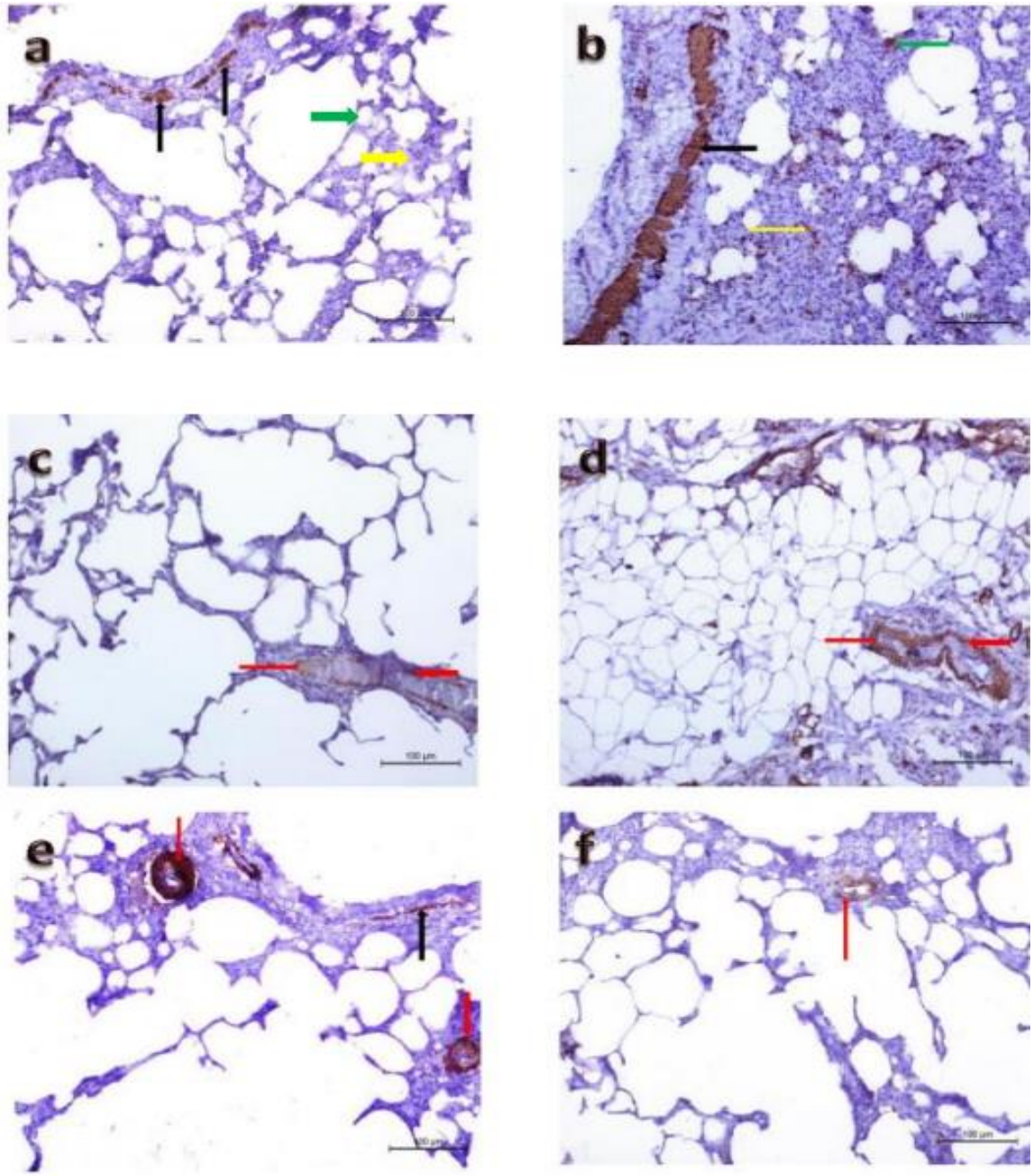

Fig (4): α SMA immunohistochemical stained sections:

A Photomicrograph of α SMA stained lung sections of (4a): groupI control group showed showed positive cytoplasmic reaction in the smooth muscles investing bronchioles (black arrows) and negative α SMA reaction in the wall of alveoli (green arrow) and interalveolar septa (yellow arrow). (4b): groupII (CP) treated group sections showed strong positive cytoplasmic reaction in the walls of alveoli (green arrow), in the walls of bronchioles (black arrows) and interalveolar septa (yellow arrow). In groupIII valsartan treated (4c) and groupVI (CP +Valsartan) (4f) showed weak cytoplasmic immunoreactivity for α SMA in the walls of blood vessel (red arrow). Lung sections in groupV (CP + DEXa) treated (4e) and groupIV (Dexa) treated (4d), showed moderate cytoplasmic immunoreactivity for αSMA in the wall of bronchiole and the walls of blood vessel (red arrow). (α SMA x200).

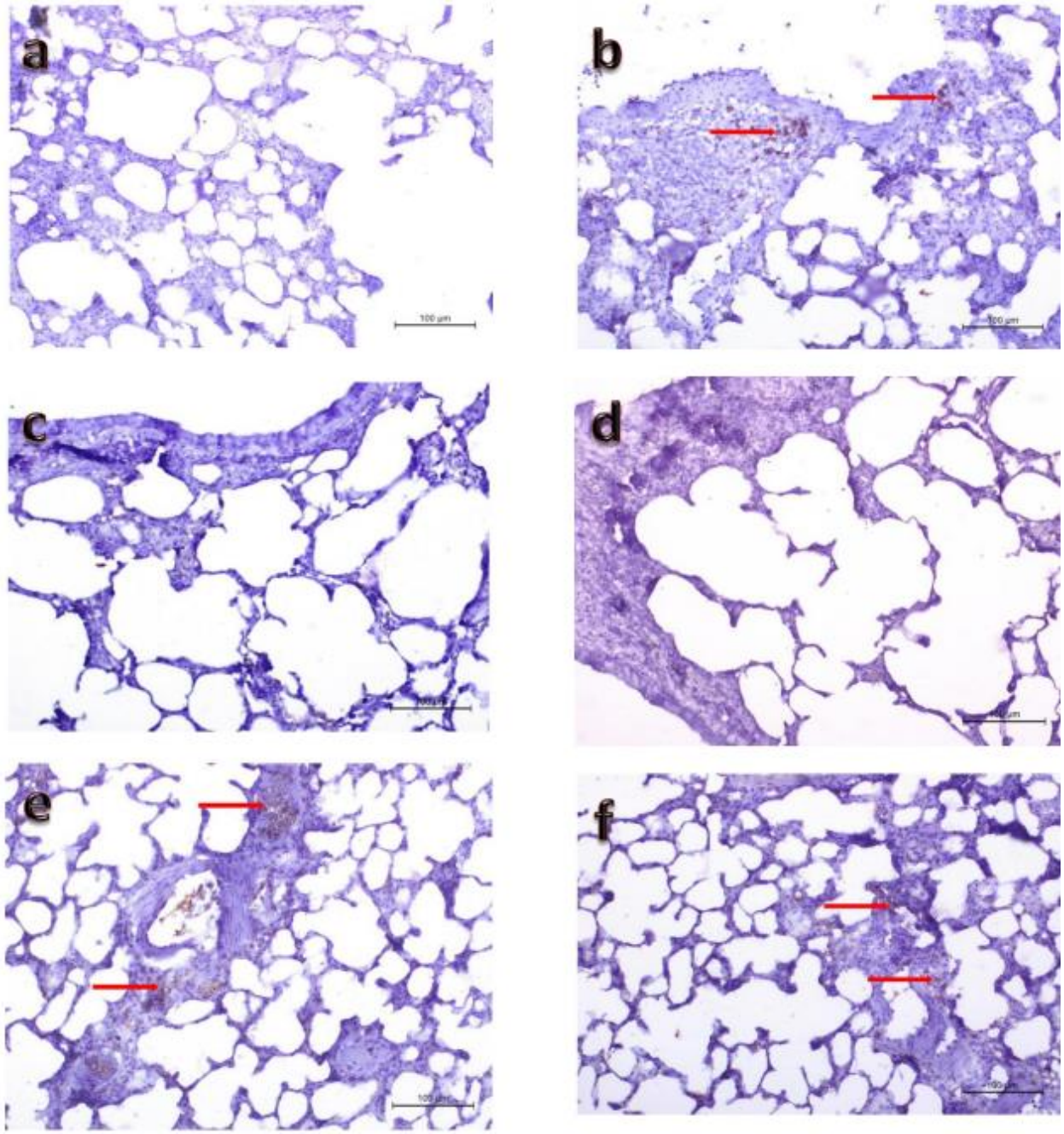

Fig (5): CD68 immunohistochemical stained sections

A Photomicrograph of CD68 stained lung sections of (5a): groupI control group showed negative CD68 alveolar macrophages in the interalveolar septum. In (5b): groupII (CP) treated group showed moderate positively stained CD68 alveolar macrophages within the interalveolar septa (red arrow). In groupIII valsartan treated (5c) and groupVI (CP +Valsartan) (5f) showed negative CD68 alveolar macrophages in the interalveolar septum. In groupV (CP + DEXa) treated (5e) and sections showed moderate positive stained CD68 alveolar macrophages in the interalveolar septa (red arrow). In groupIV (Dexa) treated (5d) sections showed few positive stained CD68 alveolar macrophages in the interalveolar septa (red arrow). (CD68 x200).

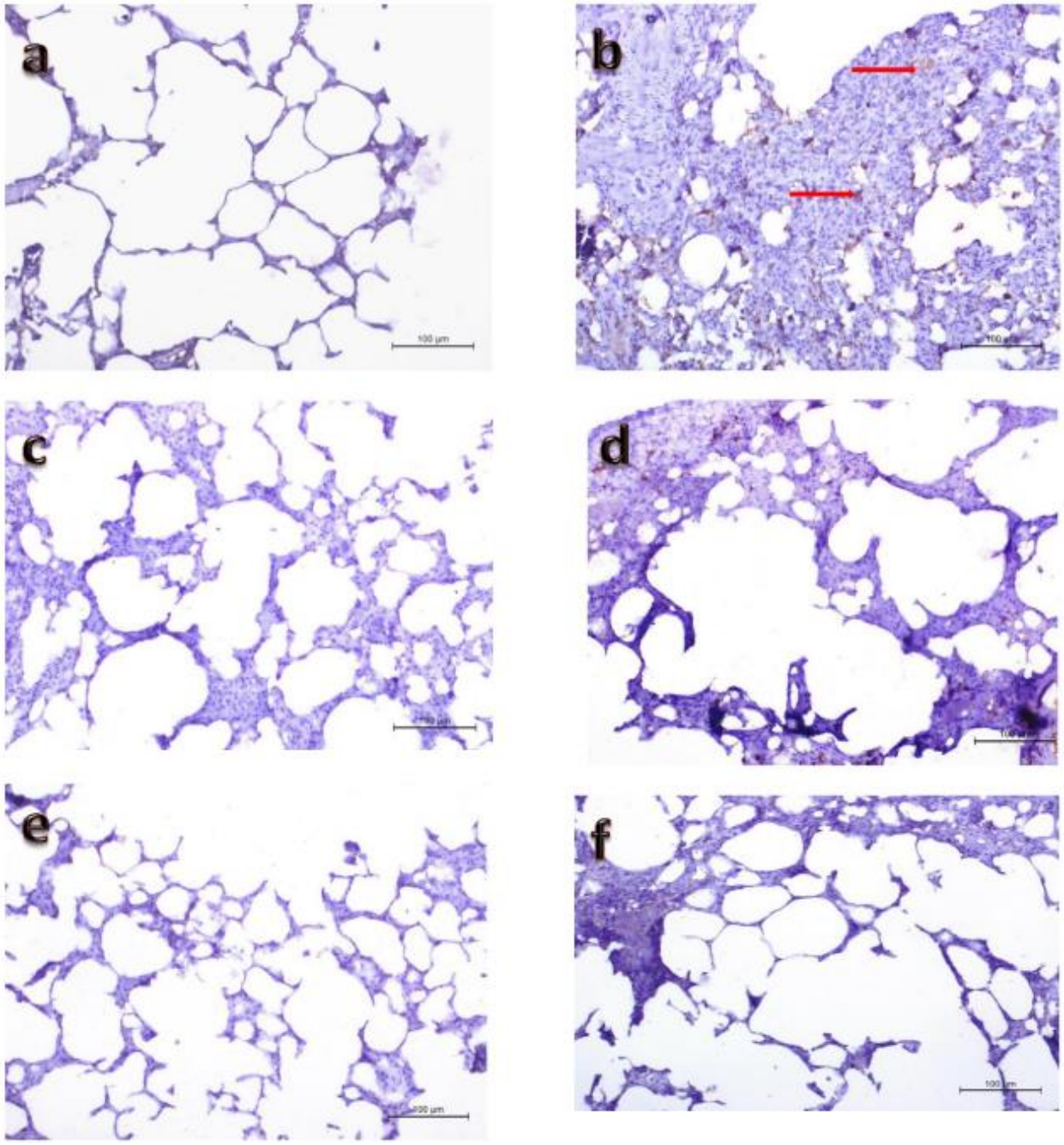

Fig (6):iNOS immunohistochemical stained sections

A Photomicrograph of iNOS stained lung sections (6a): groupI control group showed negative iNOS expression in the interalveolar septum (red arrow). In (6b): groupII (CP) treated group sections showed moderate iNOS immunoreactive cells within the interalveolar septum. In groupIII valsartan treated (6c) and groupIV (Dexa) treated (6d) sections showed negative iNOS expression in the interalveolar septum In groupV (CP + DEXa) treated (6e) and groupVI (CP +Valsartan) (6f) sections showed negative iNOS expression in the interalveolar septum. (iNos x200).

Groups / Parameters	**Alveolar thickness**	**PAS %**	**masson's trichrome%**	**SMA %**	**INOS**	**CD 68**
GpI: Control	3.97±0.449	2.10±0.434	0.54±0.078	0.44±0.078	0.42±0.045	7.75±0.854
Gp II: CP	26.11±3.331[a]	10.40±0.146[a]	7.28±0.726[a]	6.28±0.726[a]	1.41±0.124[a]	15.00±1.183[a]
GP III	3.99±0.667[b]	2.26±0.469[b]	0.64±0.064[b]	0.54±0.064[b]	0.53±0.048[b]	8.50±0.646[b]
GP IV	3.47±0.314[b]	2.17±0.356[b]	0.66±0.035[b]	0.56±0.035[b]	0.46±0.049[b]	8.00±0.817[b]
GP V	3.75±0.430[b]	6.19±0.720[b]	3.33±0.541[b]	3.43±0.541[b]	0.67±0.168[b]	8.00±0.577[b]
GP VI	4.81±0.542[b]	3.04±0.735[b]	2.72±0.222[b]	2.02±0.222[b]	0.55±0.104[b]	8.00±0.408[b]
P.value	<0.0001	<0.0001	<0.0001	<0.0001	<0.0001	<0.0001

Table (1): Statistical analysis summary of the morphometrical parameters of the lung of all experimental groups

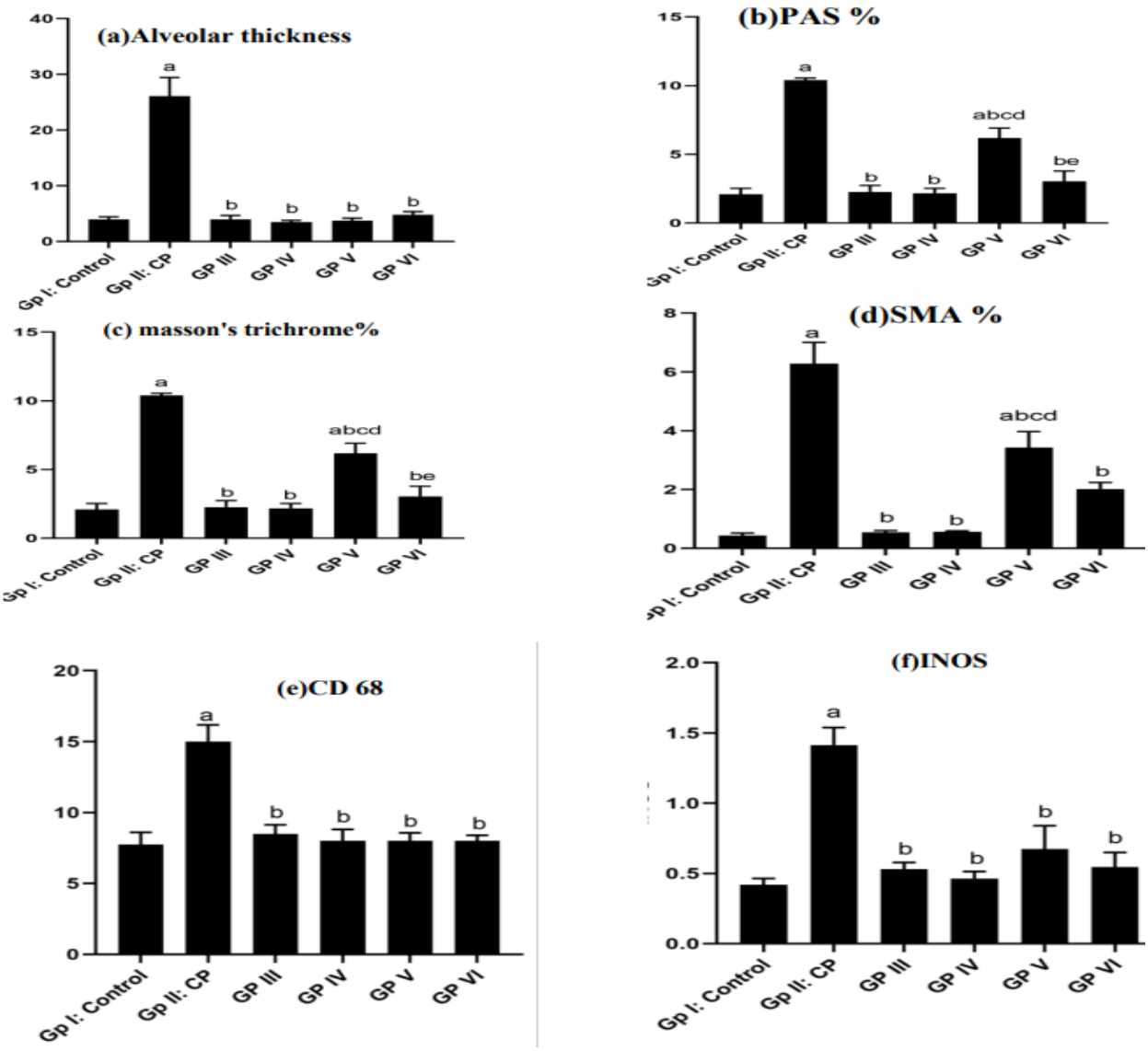

Fig (7): Histogram (a): Comparison between the mean values of the thickness of interalveolar septa in all experimental groups. Histogram (b): Comparison between the mean number of PAS-positive goblet cells per bronchiole in all experimental groups. Histogram(c): Comparison between the area percentage of masson's trichrome stained collagen fibers in all experimental groups. Histogram (d): Comparison between the area percentages of α-SMA immune-stained smooth muscle in all experimental groups. Histogram (e): Comparison between the mean number of alveolar macrophages in anti-CD68 immunostained sections in all experimental groups. Histogram (f): Comparison between the mean area percentage of positive iNOS immunoreactivity in anti-iNOS immunostained sections in all experimental groups.

3. Discussion:

Idiopathic pulmonary fibrosis (IPF) is one of the most common and aggressive forms of lung fibrosis with high mortality and morbidity. It develops without an identified underlying cause and terminates with severe affection of lung functions.

We induced IPF in our study using cyclophosphamide as it has been documented to be fast, effective, and mimic the histopathology of human IPF to a great extent [(11).]

This study is aimed to investigate the protective effect of valsartan versus DEXA as a pretreatment on Cyclophosphamide induced pulmonary fibrosis and to explore the possible mechanism that might be involved in valsartan and DEXA protective effects [(10,12)].

Light microscopic examination of lung in group II (CP treated group) showed thickening of the interalveolar septum, diffuse inflammatory cell infiltrations, with narrowing of the alveolar spaces. The mucosa of the respiratory bronchiole was irregular and detachment of the bronchiolar epithelial lining were also seen. This is in concomitant with [(11)]. This was confirmed by morphometric results as there was a significant increase in the thickness of interalveolar septa in group II compared to group I (control).

Previous studies reported that the pathophysiology of CP toxicity is due to the induced oxidative stress. The oxidative stress results in increased production of pro-inflammatory cytokines and stimulation of several signaling pathways and thus leading to inflammation and fibrosis [(5)].

As demonstrated by PAS stain, lung sections in group II (CP) showed strong PAS reaction at most of goblet cells of the epithelial lining of the bronchioles, in comparison with weak PAS reaction in the control group (group I). These findings were confirmed by the morphometric and statistical results as there was a significant increase in the number of PAS-positive goblet cells per bronchiole in group II (CP treated group) when compared to group I (control). These results could be supported by the report of **El-Sheikh et al., (2017)[(11)]** who demonstrated that one of the most pathological effects of exposure to CP was goblet cell hyperplasia and proliferation of airway epithelial cells including bronchial and bronchiolar epithelium.

The key mechanism underlying the pulmonary airway mucus hypersecretion is the production of ROS and its induced activation of epidermal growth factor

receptor (EGFR), via enhancing its kinase activity, receptor modification, and structure alteration [13].

As demonstrated by Masson's trichrome stain, group II (CP treated group) showed collagen deposition around blood vessels and also in the interalveolar septa. This was confirmed by the morphometric results as there was a significant increase in the mean area percentage of collagen fibers in group II when compared to the group I (control). This was in accordance to **Li et al., (2019) [14]** who found a significant increase in hydroxyproline level; a marker for collagen content in the CP treated lung compared to the control.

It was recorded that, fibrosis starts to develop due to activation of fibroblasts into myofibroblasts, which secrete extracellular matrix and deposit collagen [15].

Using α-SMA immunostaining, the lung sections of group II (CP) revealed many positively stained cells that were evident in the interalveolar septa in comparison to the control group. This was confirmed by the morphometric results where the mean area percentage of αSMA was significantly higher compared to that of the control group. These immunohistochemical results were also in accordance with **Schiller, H. B., et al., (2015) [15] who** found that CP treatment significantly increased the mean number of α-SMA positive myofibroblasts.

It was hypothesized that the mechanism of fibroblast stimulation relied on cytokine release by macrophages, which secrete a variety of hormone-like molecules that enhance fibroblast growth [16].

In the present study, examination of CD68 immunostained sections showed moderate positively stained CD68 alveolar macrophages within the interalveolar septa and in the lumen of alveoli, in comparison with weak CD68 expression in the control group (group I). These findings were confirmed by the morphometric and statistical results, as there was a significant increase in alveolar macrophages in anti-CD68 immuostained sections in group II (CP treated) as compared with group I control group. These results could be supported by the report of **Carthy, J. M. (2018) [17]** who demonstrated that macrophages are activators for mediator capable of regulating fibroblast proliferation and other functions that are responsible for the fibrogenic outcome.

The present study showed an infiltration of the lung tissue with inflammatory cells such as neutrophils and macrophages, and it could be assumed that the inflammatory cells especially macrophages may play an important role in such fibrosis [5].

It was hypothesized that in idiopathic pulmonary fibrosis (IPF), chronic and repetitive alveolar epithelial cell injury occurs with subsequent release of various cytokines as transforming growth factor beta (TGFβ), platelet-derived growth factor (PDGF), fibroblast growth factor (FGR) and vascular endothelial growth factor (VEGF) [18]. TGFβ was clarified to be the main contributor of disease progression [19].

In the present study, examination of iNOS immunostained sections showed moderate iNOS immunoreactive cells within the interalveolar septa in comparison with weak iNOS expression in the control group (group I). These findings were confirmed by the morphometrical and statistical results، there was a significant increase in the area percentage of iNOS staining in group II, in comparison with group I

Our study reported that alveolar epithelial cells (AECs) were exposed to oxidative damage that might be attributed to CP. This is in agreement with **Cameli, P et al., (2020)** [20] who reported that, CP upregulates Fas-Fas antigen, which is a cell surface protein that mediates oxidative damage, is sufficient to initiate a fibrotic lung reaction in mice.

Light microscopic examination of the sections of the respiratory portion of lung did not show substantial differences among rats in group I (control) ،group III (valsartan treated group) and group IV (dexamethasone treated group) and their results were similar to the normal structure which is confirmed by the morphometric and statistical results.

Concerning the results of group V (CP + Dexa) and group VI(CP +Valsartan) in the present work, H&E stained sections showed that most of alveoli and interalveolar septa restored their normal architecture in the form of nearly normal thickness of an interalveolar septum, mild cellular infiltration of the interstitium and patent alveoli. These findings were confirmed by the morphometric and statistical results. There was a significant decrease in in the thickness of interalveolar septa in group V (CP + Dexa) and group VI (CP +Valsartan) in comparison with group II (CP).

Valsartan succeeded in restoring the lung integrity by lowering oxidative stress induced by CP [21]. Also dexamethasone reduced alveolar inflammation and damage. The main mechanism of action of dexamethasone is ultimately its inhibitory effect on TGF-β level demonstrated in many studies [22].

Examination of PAS stained lung sections showed few PAS positive goblet cells in the lung bronchi. These findings were

confirmed by the morphometric and statistical results there was a significant decrease in the mean number of PAS-positive goblet cells per bronchiole in group V (CP + Dexa) and group VI (CP +Valsartan) in comparison with group II(CP treated group). There were similar findings detected by **Abdel-Latif, G. A** et al., **(2020)** [5] revealed normal reaction of few goblet cells without any evidence of increased their number.

It was hypothesized that Valsartan and Dexa cause inhibition of epidermal growth factor receptor (EGFR).Which in turn decrease goblet cell hyperplasia and proliferation [13].

Examination of Masson's trichrome stained lung sections in group V (CP + Dexa) and group VI (CP +Valsartan) showed moderate deposition of collagen fibers in the interalveolar septa. These findings were confirmed by the morphometric and statistical results there was a significant decrease mean area percentage of masson's trichrome stained collagen fiber in group V and group VI in comparison with group II.

Accordingly, the present study showed a significant reduction in the fibrotic changes of the lung in CP induced pulmonary fibrosis in case of pretreatment with valsartan 6 days before CP administration. Which is in accordance with **Kakugawa, T et al., (2004)** [23] who found that valsartan treatment significantly attenuated pulmonary fibrosis, in CP induced pulmonary fibrosis.

As regards alpha smooth muscle actin in the present study lung of rats in group V (CP + Dexa) and group VI (CP +Valsartan) showed weak cytoplasmic immunoreactivity for αSMA in the walls of alveoli and interalveolar septa, positive immunoreactivity in the walls of blood vessels. These findings were confirmed by the morphometric and statistical results as there was a significant decrease in the area percentage of alpha smooth muscle actin in group V and group VI in comparison with group II. There were similar findings detected by **Ismail, M et al., (2015)** [24].

The mechanism of the pulmonary antifibrotic effect of valsartan in the present study could be attributed to its inhibitory effect on α-SMA positive myofibroblasts, which was reported by **Kakugawa, T et al., (2004)** [23] to be the principal cell responsible for accumulation and deposition of extracellular matrix seen in pulmonary fibrosis. Through suppression of TGFβ-mediated pathways, dexamethasone decreases transformation of fibroblast into myofibrobasts and their proliferation. It also inhibits expression of α-SMA in myofibroblasts [25].

By examination of CD68 immunostained sections; it showed few positive stained CD68 alveolar macrophages in the interalveolar septum.These findings were confirmed by the morphometric and statistical results، there was a significant decrease in alveolar macrophages in anti-CD68 immuostained sections in group V (CP + Dexa) and group VI (CP +Valsartan) in comparison with group II. There were similar findings detected by **Abdel-Latif, G. A et al., (2020)** [5] who reported that valsartan pretreatment decrease number of macrophages in the interalveolar septum.

It was also hypothesized that, dexamethasone and valsartan cause inhibition of macrophage infiltration and subsequent inflammatory recruitment [26]. In the present study, immunohistochemical reaction of the lung in group V (CP + Dexa treated) and group VI (CP +Valsartan) showed few iNOS positive cells within the alveolar and interalveolar tissues, in comparison with moderate iNOS expression in the CP (group II). These findings were confirmed by the morphometric and statistical results، there was a significant decrease in the mean area percentage of iNOS staining in group V and group VI, in comparison with group II. This is further supported by the work of **Li, V. C. (2003)** [27] who reported that simultaneous administration of valsartan with CP reduced the AEC oxidative damage and pulmonary fibrosis.

Augmentation of natriuretic peptides (NPs) (especially ANP and BNP) proved many beneficial and ameliorative effects in many cardiovascular diseases, owing to its antioxidant, anti-inflammatory properties, as well as antifibrotic impact [28].

Fortunately, DEXA treatment caused marked elevation of the antioxidants Nrf2 level along with down regulation of the iNOS protein confirmed by significant decline in the area percentage of immune-positive cells for iNOS. These findings implicate that Dexa deteriorates the oxidative stress induced by CP toxicity. In alignment with our results [29] stated that DEXA deteriorates the oxidative stress induced by CP.

Histopathological data revealed that valsartan and dexamethasone exhibited a protective effect against CP-induced oxidative and inflammatory events at the lung tissue.

Unfortunately, synthetic glucocorticoid medication has been shown to cause substantial systemic side effects, especially when used long-term or at high doses. Furthermore, it lowers quality of life, reduces life expectancy and raises health-care costs [30].

4. Conclusion:

Based on our results we can conclude that:

* Dexamethasone has a protective effect on pulmonary fibrosis that developed after administration of cyclophosphamide.

* Valsartan has a more potent protective effect on cyclophosphamide induced pulmonary fibrosis as approved from the histological results, via restoring the histological architecture of lung nearly to be normal and prevent cellular damage.

Recommendations

*Further studies to clarify the effect of the use of valsartan on improvement of lung fibrosis

*Further studies on the effect of dexamethasone combined with valsartan on the treatment of lung fibrosis.

*Valsartan is recommended as a pretreatment of CP treatment rather than dexamethasone because of its many side effects on the body.

5. References:

1. Qian, P., hong Peng, C., & Ye, X. (2019). Interstitial pneumonia induced by cyclophosphamide: A case report and review of the literature. Respiratory medicine case reports, 26, 212-214.
2. John, A. E., Joseph, C., Jenkins, G., & Tatler, A. L. (2021). COVID-19 and pulmonary fibrosis: A potential role for lung epithelial cells and fibroblasts. Immunological Reviews, 302(1), 228-240.
3. Siddiqui, N., Husain, A., Chaudhry, L., Alam, M. S., Mitra, M., & Bhasin, P. S. (2011). Pharmacological and pharmaceutical profile of valsartan: a review. Journal of Applied Pharmaceutical Science, (Issue), 12-19.
4. Al-Harbi, N. O., Imam, F., Al-Harbi, M. M., Ansari, M. A., Zoheir, K. M., Korashy, H. M. & Ahmad, S. F. (2016). Dexamethasone attenuates LPS-induced acute lung injury through inhibition of NF-κB, COX-2, and pro-inflammatory mediators. Immunological Investigations, 45(4), 349-369.
5. Abdel-Latif, G. A., Elwahab, A. H. A., Hasan, R. A., ElMongy, N. F., Ramzy, M. M., Louka, M. L., & Schaalan, M. F. (2020). A novel protective role of sacubitril/valsartan in cyclophosphamide induced lung injury in rats: impact of miRNA-150-3p on NF-κB/MAPK signaling trajectories. Scientific reports, 10(1), 1-17.
6. Kiernan, John. (2015). Histological and histochemical methods. Scion publishing ltd, fifth edition 155-170.
7. Bancroft, J. D. S., Layton, C., &. Suvarna, K (Eds.). (2018). Bancroft's theory and practice of histological

techniques E-Book. Elsevier health sciences 301-319.

8. Gunnar F. Nordberg, Bruce A. Fowler, Monica Nordberg and Lars T. Friberg. (2007): Handbook on the Toxicology of Metals. Science Direct 6th edition , pp 39-64
9. Emsley, R., Dunn, G., & White, I. R. (2010). Mediation and moderation of treatment effects in randomised controlled trials of complex interventions. Statistical methods in medical research, 19(3), 237-270.
10. Tripathi, D. N. & Jena, G. B. (2008). Astaxanthin inhibits cytotoxic and genotoxic efects of cyclophosphamide in mice germ cells. Toxicol- ogy 248, 96–103.
11. El-Sheikh, A. A., Morsy, M. A. & Okasha, A. M. (2017). Inhibition of NF-kappaB/TNF-alpha pathway may be involved in the protective efect of resveratrol against cyclophosphamide-induced multi-organ toxicity. Immunopharmacol. Immunotoxicol. 39, 180–187.
12. El-Kashef, D. H. (2018). Role of venlafaxine in prevention of cyclophosphamide-induced lung toxicity and airway hyperactivity in rats. Environmental Toxicology and Pharmacology, 58, 70-76.
13. Paulsen, C. E., Truong, T. H., Garcia, F. J., Homann, A., Gupta, V., Leonard, S. E., & Carroll, K. S. (2012). Peroxide-dependent sulfenylation of the EGFR catalytic site enhances kinase activity. Nature chemical biology, 8(1), 57-64.
14. Li, L., Li, Q., Wei, L., Wang, Z., Ma, W., Liu, F., & Qian, Y. (2019). Dexamethasone combined with berberine is an effective therapy for bleomycin-induced pulmonary fibrosis in rats. Experimental and Therapeutic Medicine, 18(4), 2385-2392.
15. Schiller, H. B., Fernandez, I. E., Burgstaller, G., Schaab, C., Scheltema, R. A., Schwarzmayr, T., & Mann, M. (2015). Time-and compartment-resolved proteome profiling of the extracellular niche in lung injury and repair. Molecular systems biology, 11(7), 819.
16. Liu, T., De Los Santos, F. G., & Phan, S. H. (2017). The bleomycin model of pulmonary fibrosis. Fibrosis: Methods and Protocols, 27-42.
17. Carthy, J. M. (2018). TGFβ signaling and the control of myofibroblast differentiation: Implications for chronic inflammatory disorders. Journal of cellular physiology, 233(1), 98-106.
18. Knudsen, L., Ruppert, C., & Ochs, M. (2017). Tissue remodelling in pulmonary

fibrosis. Cell and Tissue Research, 367, 607-626.

19. Penke, L. R., & Peters-Golden, M. (2019). Molecular determinants of mesenchymal cell activation in fibroproliferative diseases. Cellular and Molecular Life Sciences, 76, 4179-4201.
20. Cameli, P., Carleo, A., Bergantini, L., Landi, C., Prasse, A., & Bargagli, E. (2020). Oxidant/antioxidant disequilibrium in idiopathic pulmonary fibrosis pathogenesis. Inflammation, 43, 1-7.
21. Vavrinec, P., H Henning, R., W Landheer, S., Wang, Y., E Deelman, L., PE van Dokkum, R., & Buikema, H. (2014). Vildagliptin restores renal myogenic function and attenuates renal sclerosis independently of effects on blood glucose or proteinuria in Zucker diabetic fatty rat. Current Vascular Pharmacology, 12(6), 836-844.
22. Rasooli, R., Pourgholamhosein, F., Kamali, Y., Nabipour, F., & Mandegary, A. (2018). Combination therapy with pirfenidone plus prednisolone ameliorates paraquat-induced pulmonary fibrosis. Inflammation, 41, 134-142.
23. Kakugawa, T., Mukae, H., Hayashi, T., Ishii, H., Abe, K., Fujii, T., ... & Kohno, S. (2004). Pirfenidone attenuates expression of HSP47 in murine bleomycin-induced pulmonary fibrosis. European Respiratory Journal, 24(1), 57-65.
24. Ismail, M., Hossain, M., Tanu, A. R., & Shekhar, H. U. (2015). Effect of spirulina intervention on oxidative stress, antioxidant status, and lipid profile in chronic obstructive pulmonary disease patients. BioMed research international, 201-215.
25. Bellaye, P. S., Yanagihara, T., Granton, E., Sato, S., Shimbori, C., Upagupta, C., & Kolb, M. (2018). Macitentan reduces progression of TGF-β1-induced pulmonary fibrosis and pulmonary hypertension. European Respiratory Journal, 52(2) 134-150.
26. Chen, J. F., Ni, H. F., Pan, M. M., Liu, H., Xu, M., Zhang, M. H., & Liu, B. C. (2013). Pirfenidone inhibits macrophage infiltration in 5/6 nephrectomized rats. American Journal of Physiology-Renal Physiology, 304(6), F676-F685.
27. Li, V. C. (2003). On engineered cementitious composites (ECC) a review of the material and its applications. Journal of advanced concrete technology, 1(3), 215-230.
28. Judge and Parminder.(2015)."Neprilysin inhibition in chronic kidney disease." Nephrology Dialysis Transplantation 30.5 :738-743.
29. Salama RM, Abd Elwahab AH, Abd-Elgalil MM, Elmongy NF, Schaalan MF.

(2020) .LCZ696 (sacubitril/valsartan) protects against cyclophosphamide-induced testicular toxicity in rats: Role of neprilysin inhibition and lncRNA TUG1 in ameliorating apoptosis. Toxicology 437:152439-152443.

30. Paragliola, R. M., Papi, G., Pontecorvi, A., & Corsello, S. M. (2017). Treatment with synthetic glucocorticoids and the hypothalamus-pituitary-adrenal axis. International journal of molecular sciences, 18(10), 2201-2209.